VIP Photoacoustic Imaging Very Important Paper

International Edition: DOI: 10.1002/anie.201508616
German Edition: DOI: 10.1002/ange.201508616

Folding Up of Gold Nanoparticle Strings into Plasmonic Vesicles for Enhanced Photoacoustic Imaging

Yijing Liu, Jie He, Kuikun Yang, Chenglin Yi, Yi Liu, Liming Nie, Niveen M. Khashab, Xiaoyuan Chen, and Zhihong Nie**

Abstract: *The stepwise self-assembly of hollow plasmonic vesicles with vesicular membranes containing strings of gold nanoparticles (NPs) is reported. The formation of chain vesicles can be controlled by tuning the density of the polymer ligands on the surface of the gold NPs. The strong absorption of the chain vesicles in the near-infrared (NIR) region leads to a much higher efficiency in photoacoustic (PA) imaging than for non-chain vesicles. The chain vesicles were further employed for the encapsulation of drugs and the NIR light triggered release of payloads. This work not only offers a new platform for controlling the hierarchical self-assembly of NPs, but also demonstrates that the physical properties of the materials can be tailored by controlling the spatial arrangement of NPs within assemblies to achieve a better performance in biomedical applications.*

Gold nanoparticles (GNPs) have been extensively explored in nanomedicine owing to their unique size and intrinsic optical properties, such as localized surface plasmon resonance and photothermal effects (i.e., the conversion of absorbed light into heat).[1] A GNP-based platform uniquely combines imaging (e.g., photothermal, photoacoustic (PA), or surface enhanced Raman scattering (SERS) imaging)[2] and therapy in one system for cancer theranostics.[2a,3] The organization of GNPs into defined nanostructures (e.g., clusters, chains, or vesicles) can further improve the performance of GNPs in nanomedicine.[4] For instance, one-dimensional (1D) chains of GNPs enhance the electromagnetic field between NP gaps by several orders of magnitude, thus giving rise to significantly improved SERS signals.[5] Moreover, the ability to tune the absorption of GNP chains enables their application in photothermal cancer imaging and therapy using near-infrared (NIR) light, which benefits from deep tissue penetration.[6]

Recently, 3D vesicular assemblies of GNPs have been used as a new platform for effective cancer theranostics.[2b,6b,7] The system not only serves as a contrast agent for bioimaging, but can also be efficiently loaded with both hydrophobic and hydrophilic drugs.[2b,7a,b,8] To achieve optimal imaging and therapeutic outcomes, the interparticle spacing within these hybrid vesicles has to be carefully tuned to maximize their absorption in the NIR range. The red shift of the plasmon peak from the visible to the NIR window depends exponentially on the ratio of the interparticle distance and the NP diameter.[7a] Although larger GNPs may give rise to stronger NIR absorption, small GNPs are usually more favorable with respect to their clearance from animal bodies.[4e] However, when the GNPs are small (< 15 nm), it becomes a challenge to tune the absorption of vesicular GNP assemblies to lie in the NIR range.

Herein, we report the stepwise hierarchical self-assembly of block copolymer (BCP) tethered GNPs (BCP-GNPs) into hollow vesicles with membranes composed of GNP strings (Figure 1). The assembly involves two critical steps: the organization of individual NPs into 1D strings and the folding up of the strings into hollow vesicles (Figure 1b). The formation of chain vesicles rather than vesicles with uniform NP distributions in the membrane (referred to as non-chain vesicles; Figure 1c) was achieved by tuning the grafting

[*] Y. J. Liu,[+] Dr. J. He,[+] K. K. Yang, Dr. C. L. Yi, Dr. Y. Liu, Prof. Z. H. Nie
Department of Chemistry and Biochemistry
University of Maryland
College Park, MD 20742 (USA)
E-mail: znie@umd.edu
Dr. L. M. Nie, Dr. X. Y. Chen
Laboratory of Molecular Imaging and Nanomedicine (LOMIN)
National Institute of Biomedical Imaging and Bioengineering (NIBIB), National Institutes of Health (USA)
E-mail: shawn.chen@nih.gov
Prof. N. M. Khashab
Smart Hybrid Materials (SHMs) Lab
Department of Chemical Sciences and Engineering
Advanced Membranes and Porous Materials Center
King Abdullah University of Science and Technology (KAUST)
Thuwal 23955-6900 (Kingdom of Saudi Arabia)
[+] These authors contributed equally to this work.

Supporting information for this article is available on the WWW under http://dx.doi.org/10.1002/anie.201508616.

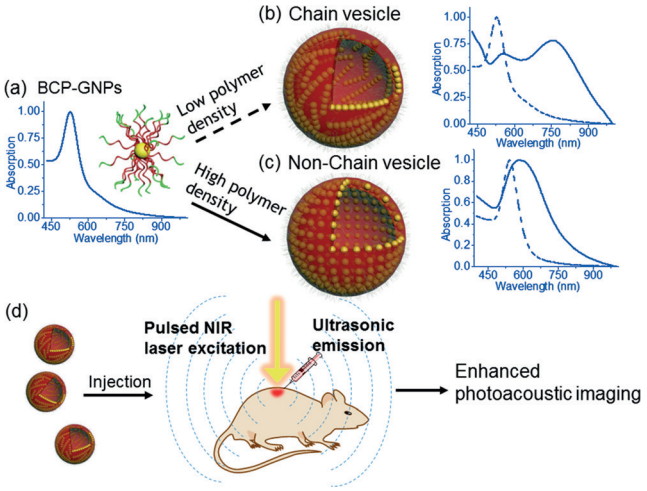

Figure 1. a–c) Self-assembly of BCP-GNPs into chain vesicles and non-chain vesicles. d) Enhanced PA imaging with chain vesicles.

density (δ) of the BCPs on the surface of the GNPs. In this way, GNP strings with strong plasmonic coupling were obtained and used as building blocks for the self-assembly of vesicles with strong absorption in the NIR window. We then demonstrated the utilization of the hybrid vesicles as PA imaging probes and drug-delivery vehicles. In in vivo imaging, the PA signal of the chain vesicles was enhanced by a factor of eight compared with that of the non-chain vesicles, while preserving their ability for the encapsulation and light-triggered release of therapeutic agents (Figure 1 d).

GNPs (13.0 ± 1.0 nm in diameter) covered with hexadecyltrimethylammonium bromide (CTAB) were modified with thiol-terminated polystyrene-*b*-poly(ethylene oxide) (PS-*b*-PEO) through an interfacial ligand exchange process that we recently developed.[7a] The PS-*b*-PEO system with a PS block of 31.6 K and a PEO block of 2 K was used throughout.[9] The δ value was controlled to be in the range of 0.03 to 0.08 chains per nm^2 by varying the BCP/GNP weight ratio during surface modification. The δ value was estimated by thermal gravimetric analysis (TGA; see the Supporting Information, Figure S1 and Table S1). The BCP-GNPs were dispersed in tetrahydrofuran (THF), and the assembly of BCP-GNPs was triggered by the solvent exchange method (i.e., the dialysis of the solution against water).[7a,8]

The formation of chain vesicles or non-chain vesicles was controlled by varying the δ value of the polymers on the GNP surface. At low δ (ca. 0.03 chains/nm^2), the assembly process led to chain vesicles with a monolayer of GNP strings in the vesicular membranes (Figure 2 a–c). When GNPs grafted with BCPs with a higher δ value (≥ 0.05 chain/nm^2) were used, non-chain vesicles were formed, and the GNPs were relatively uniformly distributed in the vesicular membranes (Figure 2 d, e). The chain vesicle has an inner cavity that is separated from the environment through a thin membrane of GNP strings. The average diameter of the chain vesicles was 520 ± 170 nm, as determined by dynamic light scattering (DLS; Figure S2). This value was slightly smaller than that determined by TEM analysis (673 ± 233 nm). This discrepancy might be due to the collapse and flattening of vesicles under vacuum conditions. The GNP strings and networks can be clearly observed in the vesicular membranes. TEM images further confirmed that the vesicles were hollow and made from a monolayer of GNP strings (Figure 2 c and Figures S3 a, S4 b). The average separation distance between GNP strings within the chain vesicles was 12.3 ± 2.2 nm. The average number of GNPs in the strings was about 6.2 GNPs per string. A close inspection of the chain vesicles indicates that the GNPs were in close contact with each other along the string; in some cases, the GNPs were even fused together (Figure 2 c, inset). The fusion of adjacent GNPs can be explained by a cold welding mechanism where gold atoms can diffuse by means of surface diffusion.[10] Moreover, attractive hydrophobic and van der Waals interactions may also facilitate the fusion of adjacent GNPs.

The average interparticle distance between GNPs within each string is 0.8 ± 0.1 nm, which is much smaller than that between GNPs in non-chain vesicles (9.0 ± 1.5 nm). The small interparticle distance within each string leads to strong NIR absorption of the chain vesicles caused by the strong coupling between adjacent GNPs.[7a,11] Whereas non-chain vesicles made from GNPs with the same size display only one absorption peak between 590 nm and 620 nm, the chain vesicles show two distinct peaks at 545 nm and 780 nm (Figure 2 f).

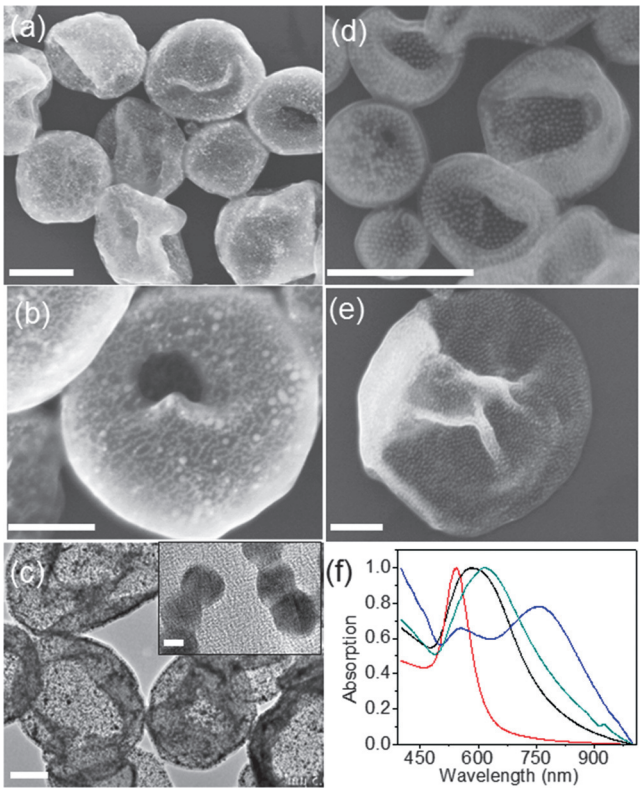

Figure 2. a–c) Representative SEM (a, b) and TEM (c) images of chain vesicles made from BCP-GNPs with 13 nm GNPs as the cores. The inset in (c) shows that several GNPs within the strings of chain vesicles are fused together. d, e) Representative SEM images of non-chain vesicles made from BCP-GNPs with 13 nm GNP cores. f) UV/Vis spectra of individual GNPs (red), non-chain vesicles (green and black), and chain vesicles (blue). The chain vesicles and two different non-chain vesicles were prepared by using BCP-GNPs with δ values of 0.03, 0.05, and 0.08 chains per nm^2, respectively. Scale bars: 500 nm in (a) and (d), 250 nm in (b) and (e), 200 nm in (c), and 5 nm in the inset of (c).

We systematically investigated the formation mechanism of the chain vesicles by UV/Vis spectroscopy and TEM imaging. Water was added (1 vol% each) into a solution of BCP-GNPs in THF in a stepwise fashion to trigger the self-assembly. At a water concentration of 5 vol%, both TEM imaging and UV/Vis spectroscopy revealed that most BCP-GNPs were present as individual NPs (Figure 3 a, b). Upon an increase in the water content to approximately 10 vol%, 1D strings of GNPs formed, as indicated by the TEM images and the appearance of a new peak at 607 nm in the UV/Vis spectrum (Figure 3 a, c). Above 20 vol% water content, all of the 1D strings rolled into chain vesicles (Figure 3 d). This process was accompanied by a further red shift of the plasmon peak. This result suggests a novel two-step hierarchical self-assembly process for the formation of NP strings from individual NPs and the subsequent assembly of NP strings into vesicles.

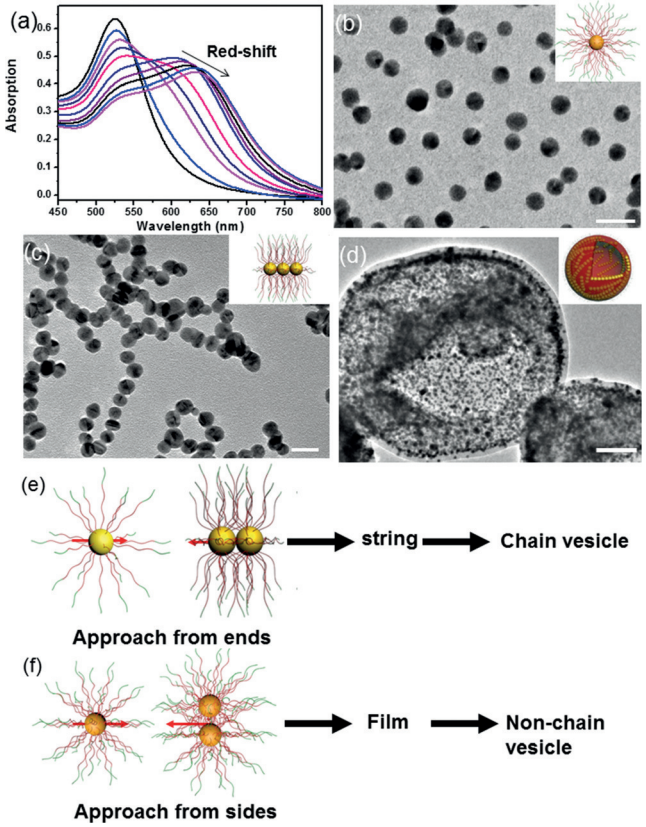

Figure 3. The mechanism and kinetics of the self-assembly of BCP-GNPs with 13 nm cores. a) UV/Vis spectra of BCP-GNPs with 13 nm cores at different water concentrations. b–d) Representative TEM images of assemblies obtained at 5, 10, and 100 vol% of water in water/THF mixtures. Scale bars: 20 nm in (b) and (c), 100 nm in (d). e, f) Mechanisms of the formation of chain (e) and non-chain vesicles (f).

The competition in the formation of chain or non-chain vesicles can be explained as follows: At low polymer δ values, as a result of the strong van der Waals forces between a pair of very closely associated GNPs, the segments of the BCP chains are squeezed out of the gaps between NP pairs, leading to a higher polymer density around the center than at the two poles of NP pairs (Figure 3e). This results in strong three-body repulsive forces at the center of NP pairs.[12] The repulsion at the center and attractive van der Waals interactions at both poles induce the formation of 1D GNP strings in the early stage of chain vesicle formation (Figure 3e). This is consistent with the fact that the separation distance between strings (ca. 12 nm) in chain vesicles is larger than that between GNP pairs in each string (ca. 0.8 nm). Unlike for most of the 1D colloidal assemblies reported previously,[5c,d,13] the electrostatic repulsion is not the dominant repulsive force in the process of string formation, which is largely due to the low dielectric constant (12.59) of the mixed solvent (10 vol% water in THF).[14] This was confirmed by a control experiment: the formation of chain vesicles was not influenced by the presence of electrolytes (0–500 mM NaCl). Upon further addition of water, the instability of the GNP strings led to their association into enclosed vesicles to minimize the interfacial tension (Figure S5). In contrast, at high δ values, the GNPs are fairly far apart in the NP pairs, which dramatically weakens the van der Waals attractions between GNPs. The steric repulsion is mainly balanced by attractive hydrophobic interactions. To maximize these interactions, individual NPs approach the clusters from the sides to form 2D thin films and eventually non-chain vesicles (Figures S5 and S7).

The linear organization of GNPs into chain vesicles results in strong NIR absorption of the assemblies, which is due to the strong coupling between the GNPs in the strings and a useful property for in vivo biomedical applications. GNPs absorb light and emit an acoustic wave that can be detected by an ultrasonic detector, thus enabling the visualization of biological tissues by so-called photoacoustic (PA) imaging.[15] PA imaging is an emerging biomedical imaging modality with large imaging depth and high spatial resolution.[16] Both chain and non-chain vesicles were used for PA imaging in vivo. Two types of vesicles containing the same amount of gold material (50 μg) were subcutaneously injected into the flank of nude mice. The injected area was irradiated with a pulsed NIR laser (780 nm with a power density of 60 mW cm^{-2}) for equal periods of time. The chain vesicle group showed an eightfold enhancement of the PA signal compared to the control group that had not be injected with PA contrast agents (Figure 4a,b). In contrast, for the non-chain vesicle group, the PA signal was only enhanced by a factor of 1.1 (Figure 4c, d). The inner cavity of the hybrid vesicles can be loaded with hydrophilic drugs, which makes the vesicles an ideal platform for drug delivery. Next, we demonstrated that GNP vesicles can be used as drug-delivery vehicles and that the release of payloads can be remotely triggered by NIR light. Rhodamine B (RhB) was encapsulated in the chain vesicles as a model drug during the self-assembly of vesicles. After the removal of free dye molecules, the RhB loaded chain vesicles were exposed to NIR light (780 nm pulsed laser, 60 mW cm^{-2}) at a time interval of 10 min. The fluorescence emission at

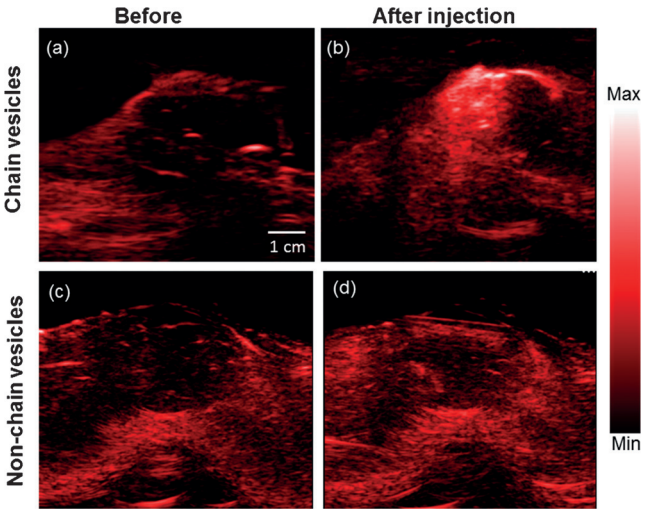

Figure 4. In vivo 2D photoacoustic imaging of mouse tissue before and after the injection of chain vesicles (a, b) or non-chain vesicles (c, d).

560 nm in solution was measured to monitor the release of RhB; it almost linearly increased with irradiation time (Figure S11). Without laser irradiation, the fluorescence intensity of the solution only slightly increased by about 13% compared with that of the laser-irradiated group. A SEM examination of the vesicles before and after irradiation showed that NIR light induced a collapse of the integrity of the chain vesicles (Figure S12). Furthermore, our vesicles are stable under physiological conditions and conditions with slightly lower pH values or higher ionic strengths. These results demonstrate the potential of chain vesicles in bioimaging and drug delivery.

In summary, we have developed a new strategy for the fabrication of GNP chain vesicles with strong NIR absorption as drug-delivery vehicles and contrast agents for photoacoustic imaging. The chain vesicles were assembled from BCP-GNPs through a new stepwise hierarchical self-assembly process, in which the competition between attractive and repulsive forces is governed by the δ value of the polymer ligands on the GNPs. The strong NIR absorption of the chain vesicles, which arises from the strong plasmon coupling between GNPs within the 1D strings, renders the chain vesicles more efficient PA imaging agents than the non-chain vesicles. This study has not only demonstrated that the properties of hybrid vesicles can be improved by engineering the arrangement of the NPs within the assemblies, but also provides fundamental information on the stepwise self-assembly of colloidal NPs for the fabrication of more complex nanostructures.

Acknowledgements

This work was funded by a National Science Foundation (NSF) CAREER award (DMR-1255377), the ACS Petroleum Research Fund (PRF 53461-DNI7), a 3M non-tenured faculty award, and the Intramural Research Program of the National Institute of Biomedical Imaging and Bioengineering, National Institutes of Health. We acknowledge support by the Maryland NanoCenter and its NispLab.

Keywords: block copolymers · gold nanoparticles · photoacoustic imaging · self-assembly · vesicles

How to cite: *Angew. Chem. Int. Ed.* **2015**, *54*, 15809–15812
Angew. Chem. **2015**, *127*, 16035–16038

[1] a) R. R. Arvizo, S. Bhattacharyya, R. A. Kudgus, K. Giri, R. Bhattacharya, P. Mukherjee, *Chem. Soc. Rev.* **2012**, *41*, 2943–2970; b) T. L. Doane, C. Burda, *Chem. Soc. Rev.* **2012**, *41*, 2885–2911.

[2] a) Z. Nie, D. Fava, E. Kumacheva, S. Zou, G. C. Walker, M. Rubinstein, *Nat. Mater.* **2007**, *6*, 609–614; b) J. He, Z. Wei, L. Wang, Z. Tomova, T. Babu, C. Wang, X. Han, J. T. Fourkas, Z. Nie, *Angew. Chem. Int. Ed.* **2013**, *52*, 2463–2468; *Angew. Chem.* **2013**, *125*, 2523–2528.

[3] a) Z. Zhang, J. Wang, C. Chen, *Theranostics* **2013**, *3*, 223–238; b) J. Song, J. Zhou, H. Duan, *J. Am. Chem. Soc.* **2012**, *134*, 13458–13469; c) Y. Liu, Y. Liu, J.-J. Yin, Z. Nie, *Macromol. Rapid Commun.* **2015**, *36*, 711–725; d) L. A. Austin, B. Kang, M. A. El-Sayed, *Nano Today* **2015**, DOI: 10.1016/j.nantod.2015.07.005; e) H. Hu, H. Duan, J. K. W. Yang, Z. X. Shen, *ACS Nano* **2012**, *6*, 10147–10155; f) J. Lin, S. Wang, P. Huang, Z. Wang, S. Chen, G. Niu, W. Li, J. He, D. Cui, G. Lu, X. Chen, Z. Nie, *ACS Nano* **2013**, *7*, 5320–5329.

[4] E. C. Dreaden, A. M. Alkilany, X. Huang, C. J. Murphy, M. A. El-Sayed, *Chem. Soc. Rev.* **2012**, *41*, 2740–2779.

[5] a) L. Wang, Y. Zhu, L. Xu, W. Chen, H. Kuang, L. Liu, A. Agarwal, C. Xu, N. A. Kotov, *Angew. Chem. Int. Ed.* **2010**, *49*, 5472–5475; *Angew. Chem.* **2010**, *122*, 5604–5607; b) A. Klinkova, H. Thérien-Aubin, A. Ahmed, D. Nykypanchuk, R. M. Choueiri, B. Gagnon, A. Muntyanu, O. Gang, G. C. Walker, E. Kumacheva, *Nano Lett.* **2014**, *14*, 6314–6321; c) H. Jaganathan, A. Ivanisevic, *J. Mater. Chem.* **2011**, *21*, 939–943; d) K. Liu, Z. Nie, N. Zhao, W. Li, M. Rubinstein, E. Kumacheva, *Science* **2010**, *329*, 197–200; e) L. Y. T. Chou, K. Zagorovsky, W. C. W. Chan, *Nat. Nanotechnol.* **2014**, *9*, 148–155; f) Y. Liu, J.-J. Yin, Z. Nie, *Nano Res.* **2014**, *7*, 1719–1730.

[6] a) C. Xi, P. M. Facal, H. Xia, D. Wang, *Soft Matter* **2015**, *11*, 4562–4571; b) G. Chen, Y. Wang, M. Yang, J. Xu, S. J. Goh, M. Pan, H. Chen, *J. Am. Chem. Soc.* **2010**, *132*, 3644–3645; c) H. Xia, G. Su, D. Wang, *Angew. Chem. Int. Ed.* **2013**, *52*, 3726–3730; *Angew. Chem.* **2013**, *125*, 3814–3818; d) H. Zhang, D. Wang, *Angew. Chem. Int. Ed.* **2008**, *47*, 3984–3987; *Angew. Chem.* **2008**, *120*, 4048–4051; e) R. M. Choueiri, A. Klinkova, H. Therien-Aubin, M. Rubinstein, E. Kumacheva, *J. Am. Chem. Soc.* **2013**, *135*, 10262–10265.

[7] a) C. Loo, A. Lowery, N. Halas, J. West, R. Drezek, *Nano Lett.* **2005**, *5*, 709–711; b) P. Huang, J. Lin, W. Li, P. Rong, Z. Wang, S. Wang, X. Wang, X. Sun, M. Aronova, G. Niu, R. D. Leapman, Z. Nie, X. Chen, *Angew. Chem. Int. Ed.* **2013**, *52*, 13958–13964; *Angew. Chem.* **2013**, *125*, 14208–14214.

[8] a) J. He, X. Huang, Y.-C. Li, Y. Liu, T. Babu, M. A. Aronova, S. Wang, Z. Lu, X. Chen, Z. Nie, *J. Am. Chem. Soc.* **2013**, *135*, 7974–7984; b) J. Song, L. Cheng, A. Liu, J. Yin, M. Kuang, H. Duan, *J. Am. Chem. Soc.* **2011**, *133*, 10760–10763.

[9] Y. Liu, Y. Li, J. He, K. J. Duelge, Z. Lu, Z. Nie, *J. Am. Chem. Soc.* **2014**, *136*, 2602–2610.

[10] J. He, Y. Liu, T. Babu, Z. Wei, Z. Nie, *J. Am. Chem. Soc.* **2012**, *134*, 11342–11345.

[11] Y. Lu, J. Y. Huang, C. Wang, S. Sun, J. Lou, *Nat. Nanotechnol.* **2010**, *5*, 218–224.

[12] a) P. K. Jain, W. Huang, M. A. El-Sayed, *Nano Lett.* **2007**, *7*, 2080–2088; b) B. M. Reinhard, M. Siu, H. Agarwal, A. P. Alivisatos, J. Liphardt, *Nano Lett.* **2005**, *5*, 2246–2252.

[13] M. Rubinstein, R. H. Colby, *Polymer physics*, Oxford University Press, Oxford, **2003**.

[14] M. Yang, G. Chen, Y. Zhao, G. Silber, Y. Wang, S. Xing, Y. Han, H. Chen, *Phys. Chem. Chem. Phys.* **2010**, *12*, 11850–11860.

[15] F. E. Critchfield, J. A. Gibson, J. L. Hall, *J. Am. Chem. Soc.* **1953**, *75*, 6044–6045.

[16] M. Xu, L. V. Wang, *Rev. Sci. Instrum.* **2006**, *77*, 041101.

[17] W. Li, X. Chen, *Nanomedicine* **2015**, *10*, 299–320.

Received: September 14, 2015
Published online: November 11, 2015

